Environmental Science
Processes & Impacts

Abiotic reduction of nitrite by Fe(II): A comparison of rates and N_2O production

Journal:	*Environmental Science: Processes & Impacts*
Manuscript ID	EM-ART-06-2021-000222.R1
Article Type:	Paper

SCHOLARONE™
Manuscripts

Environmental Significance

Abiotic reduction of nitrite (NO_2^-) by Fe(II) species (i.e., chemodenitrification) is a potentially significant source of atmospheric nitrous oxide (N_2O) emissions. We compared nitrite reduction rates for a variety of Fe(II) species under similar conditions and found that rates of reduction as well as recovery as N_2O varied significantly among a wide variety of Fe(II) species. Our results suggest that reducing environments can vary substantially in how much they contribute to N_2O emissions depending on what Fe(II) species are present. Abiotic reduction of nitrite in agricultural watersheds and soils experiencing fluctuating redox conditions may be significant sources of N_2O emissions and can occur simultaneously with biological denitrification.

Abiotic reduction of nitrite by Fe(II): A comparison of rates and N_2O production

Thomas Robinson,[†] Drew E. Latta, [†] Luiza Notini,[†] Keith E. Schilling, [‡] and Michelle M. Scherer[†]

†Department of Civil and Environmental Engineering, University of Iowa, Iowa City, Iowa 52242, United States

‡ Iowa Geological Survey, 300 Trowbridge Hall, Iowa City, IA 52242-1319, United States

Abstract

Abiotic reduction of nitrite (NO_2^-) by Fe(II) species (i.e., chemodenitrification) has been demonstrated in a variety of natural environments and laboratory studies, and is a potentially significant source of atmospheric nitrous oxide (N_2O) emissions. It is, however, unclear how chemodenitrification rates and N_2O yields vary among heterogeneous Fe(II) species under similar conditions and whether abiotic reduction competes with biological NO_2^- reduction. Here, we measured rates of NO_2^- reduction and extents of N_2O production by several Fe(II) species under consistent, environmentally relevant conditions (i.e., pH 7.0, bicarbonate buffer, and 0.1 mM NO_2^-). Nitrite reduction rates varied significantly among the heterogeneous Fe(II) species with half-lives ($t_{1/2}$) ranging from as low as an hour to over two weeks following the trend of goethite/Fe(II) ~ hematite/Fe(II) ~ magnetites > maghemite/Fe(II) > sediment/Fe(II). Interestingly, we observed no clear trend of increasing NO_2^- reduction rates with higher magnetite stoichiometry ($x = Fe^{2+} / Fe^{3+}$). Nitrogen recovery as N_2O also varied significantly among the Fe species ranging from 21% to 100% recovery. We further probed both chemodenitrification and biological denitrification in the absence and presence of added aqueous Fe(II) with a sediment collected from the floodplain of an agricultural watershed. While abiotic NO_2^- reduction by the sediment + Fe(II) was much slower than the laboratory Fe(II) species, we found near complete mass N balance during chemodenitrification, as well as evidence for both abiotic and biological NO_2^- reduction potentially occurring in the sediment under anoxic conditions. Our results suggest that in redox active sediments and soils both chemodenitrification and biological denitrification are likely to occur simultaneously, and that agricultural watersheds may be significant sources of N_2O emissions.

Introduction

Abiotic reduction of nitrite (NO_2^-) by Fe(II) (i.e., chemodenitrification) has been demonstrated for several Fe(II) species including aqueous Fe(II), Fe(II) reacted with Fe oxides, Fe minerals such as green rust, magnetite, and siderite, as well as in natural environments such as paddy soils, marine sediments and tropical peat soils.[1-4, 6-18] Some evidence suggests chemodenitrification rates may rival rates of biological denitrification[5, 13, 19] and chemodenitrification is of particular interest because nitrous oxide (N_2O) is the primary reduction product whereas biological denitrification more commonly results in a mixture of nitrogen gases, including nitrogen (N_2), nitric oxide (NO), and N_2O. [9, 20, 21] Nitrous oxide is a potent greenhouse gas (GHG) with a global warming potential (GWP) of nearly three hundred times that of carbon dioxide and it is critical to accurately predict N_2O emissions to better adapt for and mitigate climate change.[13, 22-25] While large uncertainties exist in global N_2O budgets, some estimates that suggest estuarine and coastal sediments and soils contribute ~10% to global N_2O emissions likely understate the importance chemodenitrification may have on N_2O emissions from sediments and soils.[23-28]

There is increasing evidence that chemodenitrification can result in significant N_2O fluxes from sediments and soils.[5, 9, 16, 17, 23, 29] Chemodenitrification has been shown to contribute ~ 25% of total N_2O emissions from a marine sediment[9] and up to almost 70% from a terrestrial sediment.[29] In an intertidal sediment it was even observed that abiotic and fungal pathways yielded more N_2O than microbial pathways.[23] In Iowa, high rates of N_2O emission have been observed for corn fields, however, modelled N_2O emission estimates were lower than experimental results suggesting that another process, such as chemodenitrification, may be transforming N to N_2O that is not represented within the model.[30, 31] Attempts to further refine estimates of N_2O emissions from chemodenitrification in soils and sediments using N isotopic site preference have not yet been successful,[7, 22] however, recent evidence has shown that the $\varepsilon^{18}O/\varepsilon^{15}N$ ratio may adequately differentiate between biotic and abiotic NO_2^- reduction.[13]

In addition to natural Fe containing solids, even more evidence is accumulating that chemodenitrification occurs in the presence of Fe(II) species that have been synthesized in the laboratory.[2-6, 10-12, 14, 18] Nitrite reduction has been observed when Fe(II) was initially present only as aqueous Fe(II) was (i.e., homogeneous conditions), as well in heterogeneous conditions where both aqueous Fe and Fe minerals are initially present. For initially homogeneous conditions where aqueous Fe(II) was only present at the start, Fe oxides have been observed to rapidly precipitate and increase reduction rates.[2, 6, 22] Overall, heterogeneous conditions seem to produce more rapid rates of chemodenitrification than initially homogeneous conditions.[2, 5, 7, 10-13, 18, 22] Beyond that overall trend, rates of abiotic nitrite reduction by Fe(II) vary widely among these studies ranging from complete reduction within days[2, 3, 6, 9-12, 22, 32] to only partial reduction over weeks.[4, 5, 7, 13, 14, 29] Some, however, have observed more rapid chemodenitrification rates when aqueous Fe(II) concentrations increase.[2, 5] For example, the rate of nitrite reduction in the presence of goethite almost doubled with a doubling of aqueous Fe(II) concentration which is likely influenced by the amount of Fe(II) that sorbed to the mineral surface as well as the surface area of the mineral itself.[2] Faster reduction rates were also observed with higher Fe(II) concentrations in the presence of kaolinite or goethite.[2, 10] Interestingly, similar rates were observed for goethite, lepidocrocite, and ferrihydrite that precipitated from initially homogenous conditions even after adjusting for different experimental conditions which suggests that the underlying Fe oxide may not influence chemodenitrification rates.[22]

In addition to significant variability in rates of NO_2^- reduction, there is also a large variability in the extent of nitrogen recovered, typically as N_2O. Nitrous oxide recoveries vary widely and range from ~ 7%[29] to 100%[6] recovery with most reporting 50% or less recovery.[2, 3, 5, 10, 14, 22] The missing nitrogen mass is often attributed to other potential nitrogen transformation products such as nitric oxide, ammonium, and dinitrogen gas. Few, however, have measured for any of the missing nitrogen products other than N_2O, and of these, only minimal to no nitrogen mass recoveries from these gases are observed.[2-4, 6, 10, 14, 29] One exception is at high Fe and NO_2^- concentrations, complete nitrogen mass recovery as nitric oxide (NO) and N_2O was observed which suggests the missing mass in other studies is likely to be nitric oxide.[6] Further evidence for NO as the one of the missing N products comes from N isotope tracer results where more ^{14}N was found in N_2O suggesting there is a pool of heavier ^{15}N that is likely to be found as NO.[5, 22] Another potential pool for missing nitrogen could be surface bound Fe-nitrogen complexes such as an HONO complex observed recently using ATR-FTIR[14] or a previously suggested Fe-nitrosyl compound.[2]

Despite the significant evidence for chemodenitrication as a potentially significant source of atmospheric nitrous oxide (N_2O) emission, it remains unclear how chemodenitrification rates and N_2O yields vary among heterogeneous Fe(II) species under similar conditions and whether abiotic reduction competes with biological NO_2^- reduction. Here, we measured rates of NO_2^- reduction and the extents of N_2O production by a variety of Fe(II) species under a consistent set of environmentally relevant conditions (i.e., pH 7.0, bicarbonate buffer, and low NO_2^- concentration) to simulate aerobic soils with Fe oxides that have been exposed to fluctuating redox conditions. We further probed both chemodenitrification and biological denitrification in the absence and presence of added aqueous Fe(II) with a sediment collected from the floodplain of an agricultural watershed.

Materials and Methods

Mineral synthesis and characterization. The pure Fe minerals (magnetite, hematite and goethite) used in this study were synthesized using previously developed methods adapted from Cornell and Schwertmann.[33-36] Mineral purity was confirmed using powder X-ray diffraction (XRD) (Rigaku MiniFlex II, Co K_α radiation) and ^{57}Fe Mössbauer spectroscopy.

Magnetite was prepared under anoxic conditions in a glovebox (93% N_2/7% H_2) from iron chloride salts (0.1 M $FeCl_2 \cdot 4H_2O$ and 0.2 M $FeCl_3 \cdot 6H_2O$) added in a 1:2 Fe^{2+}/Fe^{3+} ratio. The salts were dissolved in deionized (DI) water and titrated with 10 M NaOH to above pH 10.0 to precipitate magnetite. To synthesize lower stoichiometry magnetites, hydrogen peroxide (30% H_2O_2) was used to oxidize magnetite particles after precipitation. After any stoichiometry adjustments, the suspension was vacuum filtered and then freeze-dried. The freeze-dried particles were returned to the glovebox, ground in a mortar and pestle, and then sieved through a 100 mesh sieve (150 μm). Magnetite stoichiometry was measured by dissolution in 5 M HCl and quantified using the 1,10-phenanthroline method and confirmed using Mössbauer spectroscopy.[37] Magnetite stoichiometry varied from an Fe^{2+}/Fe^{3+} ratio (x) of 0.21 to 0.47.

Hematite was prepared from a solution of ferric nitrate (0.01 M $Fe(NO_3^-)_3 \cdot 9H_2O$) heated to 90 °C. Potassium hydroxide (1M KOH), sodium bicarbonate (1M $NaHCO_3$) and DI water were heated to 90 °C before their use in hematite synthesis. Ferric nitrate was added to the heated DI water, followed by the KOH and $NaHCO_3$, to create a reddish-brown suspension. The pH was adjusted to between pH 8.0 and 9.0 and heated at 90 °C for 48 hours. The synthesized hematite was washed, centrifuged, and freeze dried before being ground with a mortar and pestle and sieved using a 100 mesh sieve (150 μm).

Goethite was prepared from a 0.01 M ferric nitrate ($Fe(NO_3^-)_3 \cdot 9H_2O$) solution that had the pH raised by adding 5 M KOH. The resulting suspension was placed in an oven at 70 °C for 60 h. The goethite was washed, centrifuged, freeze-dried, ground with a mortar and pestle, and sieved using a 100 mesh sieve (150 μm).

Mössbauer samples were prepared by filtering suspended minerals through 0.2 μm nitrocellulose filters and then sealing the sample between two pieces of Kapton tape to avoid air oxidation. ^{57}Fe Mössbauer spectra were collected at 17 K in transmission mode using a constant acceleration drive spectrometer (Web Research, Inc., Edina, MN) and equipped with a closed-cycle cryostat (CCS-850

System, Janis Research Co., Wilmington, MA). The source was ^{57}Co(Rh) source at room temperature. Spectral calibration was performed using an α-Fe(0) foil which was then fit using Recoil software (Ottawa, Canada).

Collection and Characterization of Walnut Creek Sediments. Sediment was collected from floodplain alluvium in the Walnut Creek watershed located at the Neal Smith National Wildlife Refuge in Jasper, Iowa (41.557599, -93.266540) on August 1, 2019. The sediment was collected from the Gunder Member of the Holocene-age DeForest Formation, a silt loam alluvial fill deposited between about 10,500 and 4,500 B.P.[38] The floodplain area of the Walnut Creek watershed in central Iowa has been partially restored from *Phalaris arundinacea* to native sedge meadow after previous use as row crop agriculture.[39] Sediments were collected from the floodplain approximately 50 m from the current channel and at a depth of 2 to 3 m (8ft ± 1ft) using a soil sampling hand auger. At the time of collection, the water table was approximately 1.8 m but the water table fluctuates on the order of 0.5 to 1 m during the year.[39] Sediment was collected specifically from Walnut Creek because previous work has characterized the sediment (particle size, Fe content, etc.) and researchers have observed nutrient transformation of nitrogen and phosphorus by sediments collected at the site.[40-43] Immediately after collection, the sediments were vacuum sealed in plastic bags and stored in a cooler until final storage in a refrigerator at 35° F. Sediments were characterized using the Munsell soil chart before homogenization, and the sediment was characterized as a 10YR 7/1 (light gray), while the streaks of oxidation were characterized as a 7.5YR 5/8 (strong brown) before homogenization.

To determine the Fe(II) content of the collected sediment a chemical extraction with 5 M HCl was performed which extracted 13.5 mg Fe(II) g^{-1} sediment. As expected, HCl extracted more Fe than what was previously extracted with dithionite-citrate-bicarbonate (DCB) (3.8 mg Fe(II) g^{-1} sediment).[41] Quartz, kaolinite, and smectite clay minerals dominated the XRD pattern with no indication of Fe oxide minerals such as goethite, hematite, or magnetite (**Figure S1**). Mössbauer spectroscopy, however, confirmed the presence of Fe in the sediment and indicates that most of the Fe is present as Fe(III) (~96%) with Mössbauer parameters of the Fe(III) sextet consistent with goethite (**Figure S2**, **Table S1**).[33] The remaining four percent of the spectral area has parameters that are not unique to one Fe(II) species and could be indicative of several possible Fe-containing minerals including Fe(II) in Fe-containing clay minerals, green rust minerals, sorbed Fe(II), and primary rock-forming silicates.[44-49] Note that we collected Mössbauer spectra before and after autoclaving to confirm, at least for this sediment, that no observable transformation occurred (**Figure S2**) as has been reported in some previous work[32, 50].

Nitrite reduction experiments. All experiments were carried out in an anoxic glovebox and all solutions except sodium bicarbonate stocks were purged for at least 2 hours with N_2 gas prior to transfer into the glovebox. Sodium bicarbonate stock solutions were prepared by measuring out the sodium bicarbonate into 250 mL plastic containers which were then brought into the glovebox where 200 mL of degassed DI water was added to make the buffer. No significant difference was observed between initial experiments with hematite in the presence of MOPS and bicarbonate buffers (**Figure S3**). Sacrificial batch reactors were made in triplicate for each time point by first adding 75mg (5 g L^{-1}) for pure Fe oxide experiments, and 150 mg (10 g L^{-1}) for Walnut Creek sediment experiments to a 20 mL borosilicate glass vial. To begin the experiment, 15 mL of a buffer solution containing 1 mM $FeCl_2$, 0.1 mM KNO_2, and 10 mM $NaHCO_3$ at pH 7.0 ± 0.05 was added to the vials before they were crimp sealed and covered with

aluminum foil. An NO_2^- concentration of 0.1 mM was chosen to simulate the drinking water MCL for NO_2^-.[51] Covered reactor bottles were rotated end over end until sampled. To sample, the aqueous phase was filtered in the glovebox using a 0.22 μm nylon filter (Tisch Scientific, North Bend, OH) and aliquots were analyzed for Fe(II) using the 1,10 phenanthroline method.[52] Nitrite was quantified immediately after filtration using a method modified from Ridnour et al. which uses the Griess reaction to form a diazonium salt which can be quantified with UV-Vis colorimetry (Spectronic Genesys 5, Waltham, MA) at 540 nm.[53] For N_2O measurements, reactors bottles were removed from the glovebox where 100 ul of headspace was injected onto a GC-ECD equipped with a Supelco Carboxen 1010 PLOT fused silica capillary column (0.32 mm x 30 m). A splitless injection was used. The GC oven temperature was 150 °C and the flow rate for the carrier gas (He) was set at 4.7 mL min^{-1}. Experimental runs were followed by a post run where the oven temperature was increased to 200 °C

Select samples from NO_2^- reduction experiments using goethite were also tested for ammonium which has been reported as potential byproducts in other studies.[2, 4, 10, 29] Ammonium was quantified using a sodium salicylate-hypochlorite method to form indophenol and was adapted from Willis et al.[54] The indophenol formed was quantified with UV-Vis spectrophotometry at 685 nm. Iron precipitation at the elevated pH in the method was masked using 40 g L^{-1} sodium citrate ($Na_3C_6H_5O_7$). No ammonium was observed with a detection limit of (0.026 mg L^{-1}).[54, 55]

Results and Discussion

Nitrite reduction by aqueous Fe(II). To compare rates of nitrite reduction and extents of N_2O formation by various Fe(II) species, we measured NO_2^- reduction by aqueous Fe(II), Fe(II) reacted with goethite, hematite, and maghemite, and structural Fe(II) in magnetites over a consistent set of experimental conditions (0.1 mM NO_2^-, 1 mM Fe(II), pH 7.0 and 10 mM bicarbonate) (**Figure 1**). We observed no NO_2^- reduction by aqueous Fe(II) after one week despite having excess Fe(II) available to fully reduce NO_2^- to N_2O (**Figure 1A**). After about ten days, however, reduction began with complete reduction observed by three weeks with 76% of N recovered as N_2O. Based on previous work, we suspected that the onset of NO_2^- reduction coincided with the precipitation of an Fe(III) phase resulting in a transition to heterogeneous NO_2^- reduction.[2, 3, 22] To confirm the formation of a precipitate, we filtered the suspension shortly after the onset of reduction (~14 days or 336 hours) and collected a Mössbauer spectrum (**Figure S4**). The spectrum reveals two Fe sextets that are consistent with goethite and lepidocrocite similar to what has been observed previously.[3, 22] Note, that there was no evidence of siderite formation despite our conditions being supersaturated for siderite (Q, the reaction quotient, for our conditions is $10^{-8.33}$ which is greater than the K_{sp} of siderite which ranges from $10^{-10.12}$ to $10^{-12.57}$,[56] resulting in a saturation index of 2.56).

Our results are consistent with previous work that also observed slow or no reduction by aqueous Fe(II) that then transitions to more rapid reduction once an Fe precipitate forms.[2, 6, 22] Unlike previous work, however, we observed a significant lag before NO_2^- reduction began. The observed lag is most likely a result of our low NO_2^- (0.1 mM) and Fe(II) concentrations (1 mM). At these low concentrations, it is likely that some time is needed to form enough Fe(III) to result in measurable NO_2^- reduction and to observe a precipitate with Mössbauer spectroscopy. The lag with aqueous Fe(II) under our low NO_2^-, low Fe(II) conditions is consistent with earlier observations at a similar pH (6.5 and 8) and Fe(II) concentrations (0.8 and 0.6 mM) that observed little to no reduction over several hours.[2, 5] Increasing either the Fe(II) or pH resulted in significantly faster reduction. Comparing reported rates of NO_2^- reduction by aqueous Fe(II) reveals that rates are highly variable with half-lives ranging from just a few hours to almost six weeks (**Table S2**). The high variability has been noted before and may be because of large differences in initial conditions, as well as, rate of mineral precipitation and the identity of precipitated minerals.[2, 3, 6, 22] Despite the variability with aqueous Fe(II), it is clear that reduction rates become much more rapid once a mineral precipitate forms and the reduction process transitions from homogenous to heterogeneous as we observed here.[2, 3, 5, 6, 22]

Nitrite reduction by goethite and hematite with added Fe(II). To compare rates of NO_2^- reduction for Fe(II) reacted with Fe(III) oxides, we measured the reduction of NO_2^- by Fe(II) added to goethite and hematite (5 g L^{-1} oxide loading, 0.1 mM NO_2^-, 1 mM Fe(II), pH 7.0. and 10 mM bicarbonate). Nitrite was rapidly reduced when Fe(II) was added to the Fe oxides (**Figure 1B**). No reduction was observed by goethite or hematite alone (data not shown). Nitrite was completely transformed within twelve hours and ~ 60% N was recovered as N_2O. The kinetics of NO_2^- loss and N_2O production are remarkably similar for both goethite and hematite and follow first order kinetics (ln C vs t has $R^2 = 0.96$ and 0.97 respectively) with first-order rate coefficients of $k_{Gt} = 0.46 \pm 0.11$ h^{-1} and $k_{hem} = 0.36 \pm 0.10$ h^{-1} and almost identical N_2O recoveries of 57% and 58% (**Figure 2**). The rate of NO_2^- reduction by goethite and Fe(II) is significantly faster than what has been previously reported under similar pH and NO_2^- conditions.[2, 14, 22] For one study, the much slower rate is likely because they used a significantly lower goethite loading of 0.02 g L^{-1} compared to our 5 g L^{-1}. Normalizing the first-order rate coefficients by surface area gives surface-area normalized rate coefficients (k_{SA}, m^2 L^{-1} h^{-1}) that are much closer (within a factor of three) (**Table 1**).[2]

While NO_2^- reduction rates by hematite reacted with Fe(II) have not been reported, there is a strong similarity between both hematite/Fe(II) and goethite/Fe(II) NO_2^- reduction rates and N_2O recovery that is interesting, but perhaps not all that surprising as the aqueous Fe(II) concentrations over time in the goethite and hematite experiments are quite similar (See Figure S5). Furthermore, Fe(III) in both oxides has been shown to oxidize sorbed Fe(II) to result in homoepitaxial growth of the underlying oxide (goethite forms on goethite and hematite forms on hematite[47, 57] and measured redox potentials are also quite similar (and consistent with calculated thermodynamic potentials).[57-59] As expected with similar E^o values and aqueous Fe(II) concentrations, the estimated redox potentials for goethite/Fe(II) and hematite/Fe(II) are nearly identical under our conditions (-456 and -451 mV vs SHE, respectively) (**See SI for calculations**). Similar redox potentials suggest the rate of NO_2^- reduction is most likely not limited by thermodynamics. Others have also observed that the underlying oxide that formed did not significantly influence the rate of NO_2^- reduction in aqueous Fe(II) experiments.[22]

Nitrite reduction by magnetite and maghemite. To compare goethite/Fe(II) and hematite/Fe(II) with reduction of NO_2^- by structural Fe(II) in an Fe mineral, we measured NO_2^- reduction by magnetite and evaluated whether magnetite stoichiometry ($x = Fe^{2+} / Fe^{3+}$) influences NO_2^- reduction rates. We reacted three different magnetites with stoichiometries ranging from ($x = 0.21$ to 0.47) with NO_2^- and found that nearly stoichiometric magnetite ($x = 0.47$) reduced NO_2^- the fastest with a half-life of 2.5 hours which was similar to that of goethite and hematite reacted with Fe(II) (**Figure 1C**). The lower stoichiometry magnetites ($x = 0.41$ and 0.21) both reduced NO_2^- slower than the more stoichiometric magnetite but at rates quite similar to each other with half-lives of ~ 10 hours. While the more stoichiometric magnetite reduced NO_2^- faster, there is no clear trend of faster NO_2^- reduction with increasing magnetite stoichiometry (**Figure 2**). We found this somewhat surprising as we have observed both faster rates and greater extents of reduction with higher stoichiometries for the reduction of uranium, mercury, and nitroaromatic compounds.[34, 60-62] Given the similar NO_2^- reduction rates for magnetites of varying stoichiometry as well as goethite and hematite reacted with Fe(II) one possible explanation is that the reduction of NO_2^- by magnetites may not be thermodynamically limited, but, is instead limited by mass transport (e.g., diffusion) or by complexation kinetics (such as formation of a nitroso-iron surface complex).[2, 5] A mass transport, or complexation kinetic limitation on NO_2^- reduction by varying stoichiometric magnetites is supported by an almost ten-fold increase of the rate when the magnetite loading is doubled (from 5 to 10 g L^{-1}) (**Figure 3A**).

Regardless of magnetite stoichiometry, it is notable that the rates of NO_2^- reduction we measured are markedly faster than those previously reported. Our first-order rate coefficients for magnetite (k_{magn}) ranged from $5.4 \pm 0.9 \times 10^{-2}$ to $2.8 \pm 0.3 \times 10^{-1}$ h^{-1} which is two orders of magnitude faster than previously observed ($6.0 \pm 0.06 \times 10^{-4}$ to $1.1 \pm 0.4 \times 10^{-3}$ h^{-1}) at reasonably similar pH values (6.5 and 7.5 compared to 7.0 for our data)[4]. We also observed ~ 25% N recovery as N_2O whereas negligible recovery was previously observed (0.004%).[4] The magnetites used in our experiments, however, had a surface area ~ 40 times higher (~ 62 ± 8 m^2 g^{-1})[34] than the surface area (1.54 ± 0.18 m^2 g^{-1}) used in the previous work.[4] Normalizing for surface-area and solids loading results in surface-area normalized rate coefficients (k_{SA}) that are within an order of magnitude to previously reported rates (**Table S2**). There was also significantly less N recovery as N_2O with the magnetites (~ 25%) compared to goethite/Fe(II) and hematite/Fe(II) (~ 60%). To test whether N_2O would continue to form, we ran a longer duration experiment (two weeks) with a ten-fold increase in NO_2^- concentration (to 1 mM). The N mass balance immediately dropped and continued to do so for about two days (to about 64%) after which it steadily increased as more N_2O formed until just over 90% of the N was accounted for by N_2O (**Figure 3B**). The kinetic profile is indicative of an intermediate species that is reduced more slowly than NO_2^- and is consistent with multiple other observations of a missing intermediate N pool, such as nitric oxide (NO).[2, 4-6]

We were also interested in comparing maghemite reacted with Fe(II) with the magnetites, as maghemite has the same spinel structure as magnetite but contains no Fe(II) (i.e., $x = 0$). Maghemite reacted with Fe(II) reduced NO_2^- almost ten-fold slower ($k_{magh} = 1.0 \pm 0.2 \times 10^{-2}$ h^{-1}) compared to the magnetites as well as goethite/Fe(II) and hematite/Fe(II) (**Figure 1C**). Earlier work has shown that Fe(II) reacted with magnetite is oxidized at the surface and increases structural Fe(II) in magnetite and increases the stoichiometry.[34] We suspected something similar occurred when maghemite was reacted with Fe(II) and confirmed this by reacting ~8 mM $^{56}Fe(II)$ with maghemite and observing a distinct shift in the Mössbauer spectra from maghemite ($x = 0$) to non-stoichiometric magnetite ($x = 0.13$) (**Figure S6 see SI for calculations**). These findings suggest that maghemite and magnetite in soils may compete for electrons from Fe(II) that could otherwise reduce NO_2^- which may explain the ten-fold slower reduction rate. A similar competition for electrons from Fe(II) was recently observed for hexachloroethane (HCA) reduction by Fe(III)-bearing clay minerals.[63] These results suggest that NO_2^- reduction by Fe(II) may be influenced by the capacity of the underlying soils or sediments to accept and possibly compete for electrons from Fe(II).

Nitrite reduction by an Fe-containing sediment collected from an agricultural watershed. To explore NO_2^- reduction rates and the extent of N_2O production by an Fe containing sediment that is thought to act as a "hot spot" for denitrification, we collected sediment samples from the floodplain of a restored native prairie after decades of being used for row crop agriculture.[39-42, 64, 65] We ran a series of experiments to probe both chemodenitrification and biological denitrification in the absence and presence of added aqueous Fe(II) (**Figure 4**). To evaluate whether Fe(II) in the sediment abiotically reduced NO_2^-, we autoclaved the sediment and reacted it with 0.1 mM NO_2^- for three weeks. Despite the presence of enough Fe(II) in the sediment to reduce almost half (**~48% See SI for calculations)** of the added NO_2^- to N_2O, we observed negligible loss of NO_2^- or production of N_2O (**Figure 4A**). A Mössbauer spectrum collected of the sediment suggests Fe is present in clays in the sediments consistent with previous characterization these clays.[63] Limited reduction of NO_2^- by Fe(II) in the autoclaved sediment is consistent with previous work that has observed chemodenitrification by structural Fe in Fe containing clays *only* when the Fe content in the clay is much higher than what was measured for the Walnut Creek sediment.[5] More specifically, NO_2^- reduction was observed for a nontronite (approximately 37% Fe), but no reduction was observed for either an illite clay (approximately 1.6% Fe), or a montmorillonite clay (approximately 3.7% Fe) alone which suggests that the presence of aqueous Fe(II) may be required for low Fe containing clays to reduce NO_2^-.[5]

Addition of aqueous Fe(II) to the autoclaved sediments resulted in a significant amount of NO_2^- reduction with 60% of the NO_2^- reduced over three weeks, and near complete N recovery as N_2O (99 ± 2%) (**Figure 4C**). Substantial chemodenitrification by Walnut Creek sediment in the presence of Fe(II) is consistent with an increasing number of observations of chemodenitrification by sediments and soils after the addition of, or in the presence of, Fe(II).[7, 9, 13, 29] The rate of reduction by the autoclaved sediment/Fe(II) is notably slower ($t_{1/2}$ = 385 h) than what we observed for the Fe(III) oxides with Fe(II) as well as the magnetites (**Figure 2**). Interestingly however, the N mass balance throughout the experiment was near complete with no indication of a missing N pool as is often observed by others,[2-5, 22] and we also observed here for magnetite, goethite/Fe(II), and hematite/Fe(II) (**Figure 2**). Near complete mass balance throughout suggests that if there was an intermediate, such as NO, that reduction of the intermediate to N_2O was as fast or faster than reduction of NO_2^- to the intermediate consistent with previous work that suggested a complex network of competing pathways based on N and O isotope effects.[2, 5, 7, 13, 22] It also suggests that at least one of the parallel pathways previously suggested (NO reduction to N_2) is not occurring here.[2] Observing chemodenitrification in a sediment with a history of agricultural activity suggests that chemodenitrification can occur even in sediments that are likely to be strongly acclimated to

biological denitrification because of the high nitrogen loading. Further, the high N loadings might be expected to exceed the capacity of the Fe(II) in the sediment to abiotically reduce nitrite. These observations extend beyond agricultural soils and suggest that chemodenitrification may occur if there are conditions that bring nitrite in contact with Fe(II), for example during a precipitation-induced flushing event.

To compare chemodenitrification with biological denitrification, we reacted sediment that had not been autoclaved with NO_2^- under the same conditions. In the absence of Fe(II), we observed a kinetic profile consistent with biological reduction where we saw a lag followed by rapid loss of NO_2^- with limited N recovery as N_2O (**Figure 4B).** The kinetic profile as well as absence of N_2O is consistent with biological denitrification with N_2 gas as the likely final reduction product.[9, 20, 21] In the presence of Fe(II) added to the sediment, it appears that a mix of chemodenitrification and biological denitrification occurs as initial reduction kinetics seem similar to when autoclaved sediment and Fe(II) were used. (**Figure 4D**). Appreciable N_2O (23% of N) is only detected for one time point in one of the reactors whose NO_2^- concentrations dropped at a later time point. Additionally, it is important to note that biotic reduction of N_2O may contribute to the lack of measured N_2O from these experiments as N_2O produced by chemodenitrification may potentially have been reduced by microbes present in the unsterilized sediment.[24] Evidence for both abiotic and biological processes occurring has also been observed in paddy soils, intertidal sediments, and oceanic sediments.[7, 9, 13, 23, 29]

Our results suggest abiotic reduction of nitrite in agricultural watersheds and soils experiencing fluctuating redox conditions may be a significant source of N_2O emissions and can occur simultaneously with biological denitrification. Abiotic nitrite reduction may predominate under conditions where the concentration of organic electron donor for complete denitrification is limited or of low quality but ample Fe(II) exists in groundwater (here, H_2 was present as a donor). Such abiotic reduction could be common under fluctuating conditions where nitrate and nitrite containing waters mix with anoxic groundwater. In other environments, abiotic denitrification may also occur at interfaces such as those that occur between fine-grained and clayey sediments and coarser textured sediments or at the interface between high-permeability joints or ped faces in soils and low permeability sediments supporting fully anoxic conditions. Evidence suggests such reactions could occur in Iowa (and other glaciated landscapes) underlain by jointed till sediments.[66, 67]

Conflicts of Interest

The authors declare that there are no known conflicts of interest that may have influenced the work presented here.

Acknowledgements

This material is based upon work supported by the National Science Foundation (NSF) Division of Graduate Education (DGE) Grant No. 1633098 and through the NSF Division of Chemistry Grant No. 1708467. Additionally, the authors acknowledge Olivia Felber for preliminary work she performed as part of this project.

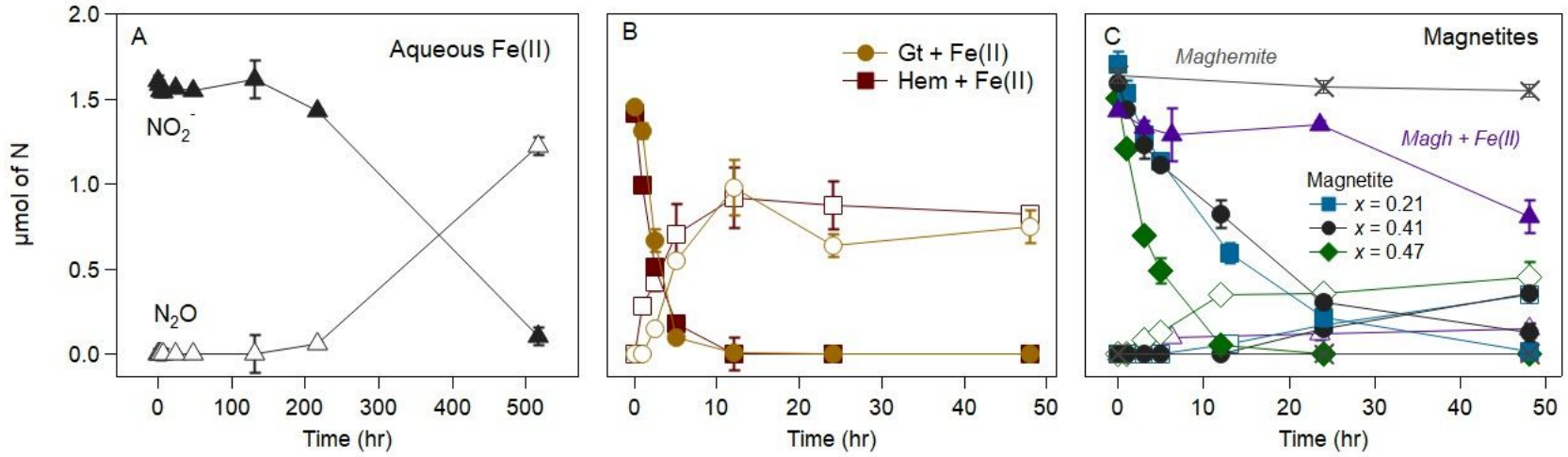

Figure 1. Kinetics of nitrite reduction (closed markers) and nitrous oxide formation (open markers) in the presence of various Fe(II) species. Left panel (A) is 1 mM aqueous Fe(II) in the absence of an initial Fe oxide. Middle panel (B) is goethite (Gt), and hematite (Hem) in the presence of 1 mM Fe(II). Right panel (C) is three different magnetites with varying stoichiometries (x = Fe(II) / Fe(III)) in the absence of Fe(II), as well as, maghemite (x = 0) alone and maghemite reacted with 1 mM Fe(II). Error bars represent average and standard deviation from triplicate reactors. **Experimental conditions:** 5 g L^{-1} Fe oxide, 1.0 mM $FeCl_2$, 0.1 mM NO_2^-, 10 mM $NaHCO_3$, initial pH 7.0.

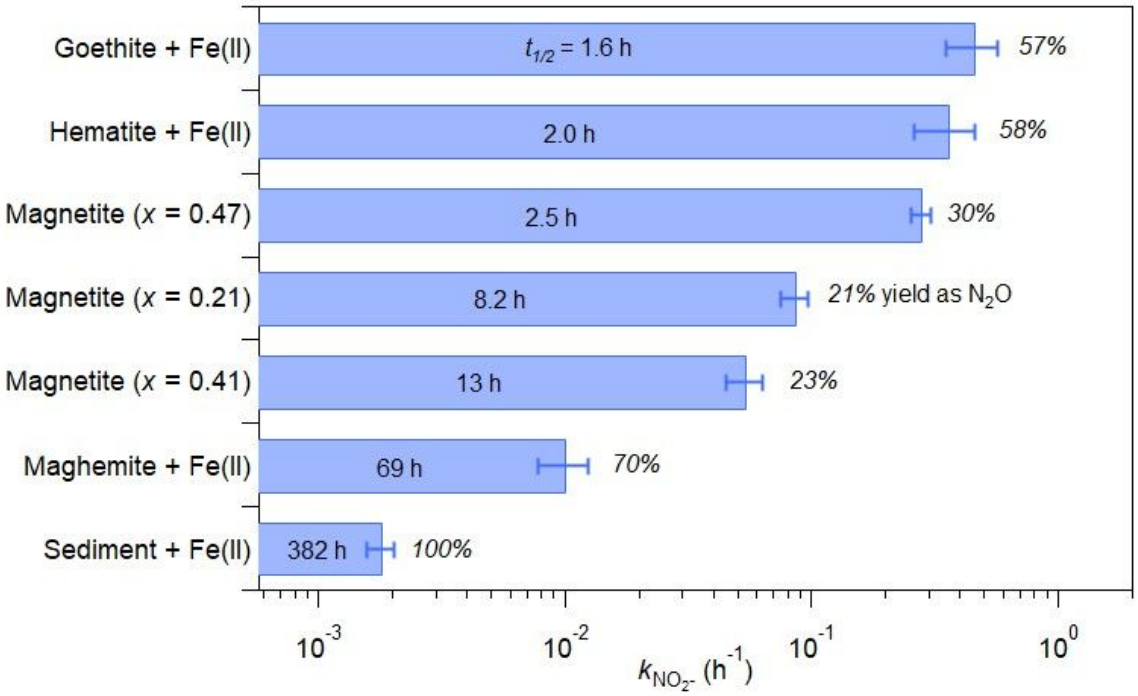

Figure 2. Comparison between first-order reduction rate coefficients for nitrite reduction (*k*) by different Fe containing oxides and sediments. The percent value after each bar represents the nitrogen mass recovered as nitrous oxide. The calculated half-lives for each rate coefficients are reported within each bar. Error bars represent the average and standard deviation from triplicate reactors. Note, aqueous Fe(II) is not included as it does not follow first order kinetics. For comparison, a half-life calculated using zero order kinetics after the observed lag in the aqueous Fe(II) data had a half-life of 169 h and 76% of the nitrogen was recovered as nitrous oxide. **Experimental conditions:** 5 g L^{-1} Fe oxide or 10 g L^{-1} sediment, 1.0 mM $FeCl_2$, 0.1 mM NO_2^-, 10 mM $NaHCO_3$, initial pH 7.0.

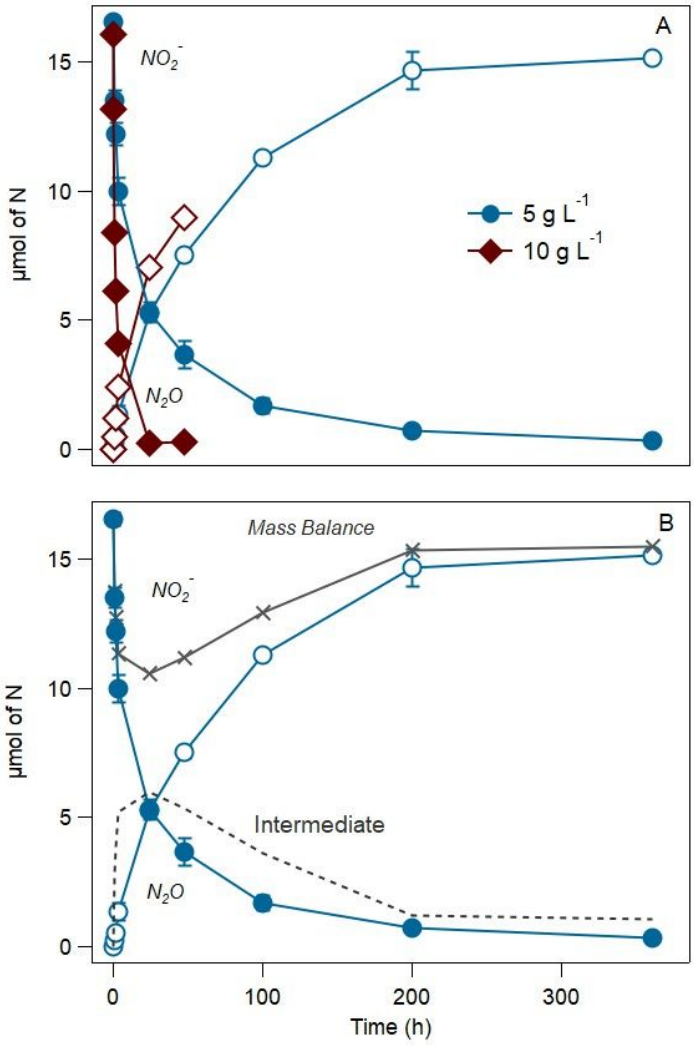

Figure 3. Kinetics of nitrite reduction (closed markers) and nitrous oxide formation (open markers) by 5 and 10 g L^{-1} magnetite (x = 0.47) (top). The 5 g L^{-1} magnetite (x = 0.47) data has been copied and a nitrogen mass balance and theoretical intermediate have been added (bottom). The intermediate (grey dashed line) represents an estimated intermediate mass and was calculated as the inverse of the mass balance (grey x markers) for the experiment. Error bars represent the average and standard deviation

from triplicate reactors. **Experimental conditions:** 5 or 10 g L^{-1} magnetite (x = 0.47), 1 mM NO_2^-, 20 mM MOPS, initial pH 7.0

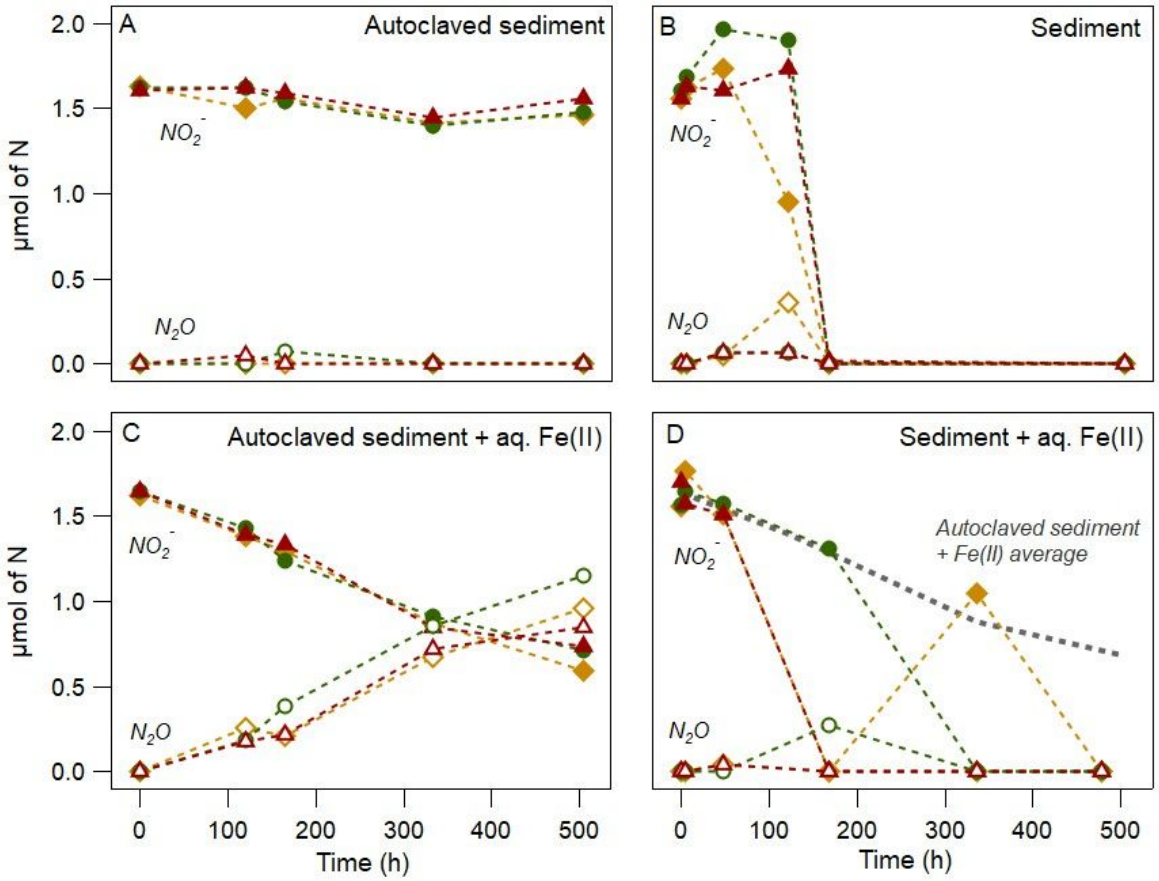

Figure 4. Kinetics of nitrite reduction (closed markers) and nitrous oxide formation (open markers) by autoclaved (left two panels A & C) and non-autoclaved (right two panels B & D) Walnut Creek sediment in the absence (top two panels A & B) and presence (bottom two panels C & D) of aqueous Fe(II). The dashed grey line in panel D represents the average NO_2^- reduction by autoclaved sediment in the presence of Fe(II) (panel C) to guide the eye. All conditions were conducted in triplicate (three colors) with sacrificial reactors punctured for nitrite samples, and then punctured for a headspace extraction. **Experimental conditions:** 10 g L^{-1} sediment, 1.0 mM $FeCl_2$, 0.1 mM NO_2^-, 10 mM $NaHCO_3$, initial pH 7.0.

Experiment	k_{obs}[a] (h^{-1})	k_M[b] ($L\ g^{-1}\ h^{-1}$)	k_{SA}[c] ($m^2\ L^{-1}\ h^{-1}$)	SA[d] ($m^2\ g^{-1}$)	$t_{1/2}$ (h)	R^2	n[e]	Initial solids loading ($g\ L^{-1}$)	Initial NO_2^- (mM)	Initial Fe(II) (mM)	Sorbed Fe(II) (mM)	Final Fe(II) (mM)	Buffer	N recovery[f]
Goethite + Fe(II)[g]	$4.6 \pm 1.1 \times 10^{-1}$	9.2×10^{-2}	2.7×10^{-3}	34	1.5	0.957	4	5	0.1	1.1	0.67	0.22	10 mM $NaHCO_3$	57%
Hematite + Fe(II)[g]	$3.6 \pm 1.0 \times 10^{-1}$	7.2×10^{-2}	2.4×10^{-3}	30	2.0	0.971	4	5	0.09	0.78	0.21	0.15	10 mM $NaHCO_3$	58%
Magnetite ($x = 0.47$)[g]	$2.8 \pm 0.26 \times 10^{-1}$	5.6×10^{-2}	9.0×10^{-4}	62	2.5	0.992	5	5	0.1	-[g]	-	-	10 mM $NaHCO_3$	30%
Magnetite ($x = 0.21$)[g]	$8.6 \pm 1.1 \times 10^{-2}$	1.7×10^{-2}	2.8×10^{-4}	62	8.1	0.998	7	5	0.11	-	-	-	10 mM $NaHCO_3$	21%
Magnetite ($x = 0.41$)[g]	$5.4 \pm 0.9 \times 10^{-2}$	1.1×10^{-2}	1.7×10^{-4}	62	12.8	0.971	7	5	0.11	-	-	-	10 mM $NaHCO_3$	23%
Magnetite ($x = 0.47$)[g]	1.5×10^{-2}	3.1×10^{-3}	4.9×10^{-5}	62	45.3	0.927	8	5	1.1	-	-	-	20 mM MOPS	93%
Magnetite ($x = 0.47$[fg]	1.7×10^{-1}	1.7×10^{-2}	5.4×10^{-4}	62	4.2	0.786	7	10	1.1	-	-	-	20 mM MOPS	56%
Maghemite + Fe(II)[g]	$1.0 \pm 0.23 \times 10^{-2}$	2.0×10^{-3}	-	-	69.3	0.772	5	5	0.09	0.66	0.64	0.02	10 mM $NaHCO_3$	70%
Sediment + Fe(II)[g]	$1.8 \pm 0.23 \times 10^{-3}$	1.8×10^{-4}	-	-	381.8	0.979	5	10	0.11	0.73	0.73	0.01	10 mM $NaHCO_3$	100%
Aqueous Fe(II)[g]	4.1×10^{-3}	-	-	-	169.0[i]	n.a	3	n.a	0.11	0.92	-	0.56	10 mM $NaHCO_3$	76%

[a] k_{obs} is the first order rate coefficient determined by fitting n points of a ln(Concentration) vs. time plot.

[b] k_M is the first order rate coefficient normalized to the solids loading.

[c] k_{SA} is the first order rate coefficient normalized to the surface area.

[d] Surface areas are estimates based on reported values for minerals previously synthesized in our lab

[e] n is the number of data points used to determine the first order rate coefficient (k_{obs}).

[f] Nitrogen mass balance recovery at final time point.

[g] All experiments began at an initial pH of 7.0 ± 0.2

[h] Dashed line signifies not applicable

[i] Half-life calculated using zero order kinetics starting after approximately 200 hours. All N recovered as N_2O

Table 1. Rate constants for nitrite reduction by a variety of Fe minerals.

References:

1. M. J. Alowitz and M. M. Scherer, Kinetics of Nitrate, Nitrite, and Cr(VI) Reduction by Iron Metal, *Environmental Science & Technology*, 2002, **36**, 299-306.
2. C. Buchwald, K. Grabb, C. M. Hansel and S. D. Wankel, Constraining the role of iron in environmental nitrogen transformations: Dual stable isotope systematics of abiotic NO2− reduction by Fe(II) and its production of N2O, *Geochimica et Cosmochimica Acta*, 2016, **186**, 1-12.
3. D. Chen, X. Yuan, W. Zhao, X. Luo, F. Li and T. Liu, Chemodenitrification by Fe(II) and nitrite: pH effect, mineralization and kinetic modeling, *Chemical Geology*, 2020, **541**, 119586.
4. P. Dhakal, C. J. Matocha, F. E. Huggins and M. M. Vandiviere, Nitrite Reactivity with Magnetite, *Environmental Science & Technology*, 2013, **47**, 6206-6213.
5. K. Grabb, C. Buchwald, C. Hansel and S. Wankel, A dual nitrite isotopic investigation of chemodenitrification by mineral-associated Fe(II) and its production of nitrous oxide, *Geochimica et Cosmochimica Acta*, 2016, **196**.
6. M. J. Kampschreur, R. Kleerebezem, W. W. de Vet and M. C. van Loosdrecht, Reduced iron induced nitric oxide and nitrous oxide emission, *Water Res*, 2011, **45**, 5945-5952.
7. R. Margalef-Marti, R. Carrey, J. A. Benito, V. Marti, A. Soler and N. Otero, Nitrate and nitrite reduction by ferrous iron minerals in polluted groundwater: Isotopic characterization of batch experiments, *Chemical Geology*, 2020, **548**, 119691.
8. J. T. Moraghan and R. J. Buresh, Chemical Reduction of Nitrite and Nitrous Oxide by Ferrous Iron, *Soil Science Society of America Journal*, 1977, **41**, 47-50.
9. J. M. Otte, N. Blackwell, R. Ruser, A. Kappler, S. Kleindienst and C. Schmidt, N2O formation by nitrite-induced (chemo)denitrification in coastal marine sediment, *Scientific Reports*, 2019, **9**, 10691.
10. S. Rakshit, C. J. Matocha, M. S. Coyne and D. Sarkar, Nitrite reduction by Fe(II) associated with kaolinite, *International Journal of Environmental Science and Technology*, 2016, **13**, 1329-1334.
11. J. Sørensen and L. Thorling, Stimulation by lepidocrocite (7-FeOOH) of Fe(II)-dependent nitrite reduction, *Geochimica et Cosmochimica Acta*, 1991, **55**, 1289-1294.
12. Y.-L. Tai and B. A. Dempsey, Nitrite reduction with hydrous ferric oxide and Fe(II): Stoichiometry, rate, and mechanism, *Water Research*, 2009, **43**, 546-552.
13. R. Benaiges-Fernandez, F. G. Offeddu, R. Margalef-Marti, J. Palau, J. Urmeneta, R. Carrey, N. Otero and J. Cama, Geochemical and isotopic study of abiotic nitrite reduction coupled to biologically produced Fe(II) oxidation in marine environments, *Chemosphere*, 2020, **260**, 127554.
14. P. Dhakal, M. S. Coyne, D. H. McNear, O. O. Wendroth, M. M. Vandiviere, E. M. D'Angelo and C. J. Matocha, Reactions of nitrite with goethite and surface Fe(II)-goethite complexes, *Science of The Total Environment*, 2021, **782**, 146406.
15. S. Buessecker, K. Tylor, J. Nye, K. E. Holbert, J. D. Urquiza Muñoz, J. B. Glass, H. E. Hartnett and H. Cadillo-Quiroz, Effects of sterilization techniques on chemodenitrification and N2O production in tropical peat soil microcosms, *Biogeosciences*, 2019, **16**, 4601-4612.
16. V. A. Samarkin, M. T. Madigan, M. W. Bowles, K. L. Casciotti, J. C. Priscu, C. P. McKay and S. B. Joye, Abiotic nitrous oxide emission from the hypersaline Don Juan Pond in Antarctica, *Nature Geoscience*, 2010, **3**, 341-344.
17. B. Peters, K. L. Casciotti, V. A. Samarkin, M. T. Madigan, C. A. Schutte and S. B. Joye, Stable isotope analyses of NO2−, NO3−, and N2O in the hypersaline ponds and soils of the McMurdo Dry Valleys, Antarctica, *Geochimica et Cosmochimica Acta*, 2014, **135**, 87-101.
18. S. Rakshit, C. J. Matocha and M. S. Coyne, Nitrite Reduction by Siderite, *Soil Science Society of America Journal*, 2008, **72**, 1070-1077.

19. N. Y. N. Lim, Å. Frostegård and L. R. Bakken, Nitrite kinetics during anoxia: The role of abiotic reactions versus microbial reduction, *Soil Biology and Biochemistry*, 2018, **119**, 203-209.
20. N. D. McTigue, W. S. Gardner, K. H. Dunton and A. K. Hardison, Biotic and abiotic controls on co-occurring nitrogen cycling processes in shallow Arctic shelf sediments, *Nature communications*, 2016, **7**, 13145-13145.
21. T. A. Doane, The Abiotic Nitrogen Cycle, *ACS Earth and Space Chemistry*, 2017, **1**, 411-421.
22. L. C. Jones, B. Peters, J. S. Lezama Pacheco, K. L. Casciotti and S. Fendorf, Stable Isotopes and Iron Oxide Mineral Products as Markers of Chemodenitrification, *Environmental Science & Technology*, 2015, **49**, 3444-3452.
23. S. D. Wankel, W. Ziebis, C. Buchwald, C. Charoenpong, D. de Beer, J. Dentinger, Z. Xu and K. Zengler, Evidence for fungal and chemodenitrification based N2O flux from nitrogen impacted coastal sediments, *Nature Communications*, 2017, **8**, 15595.
24. K. Butterbach-Bahl, M. Baggs Elizabeth, M. Dannenmann, R. Kiese and S. Zechmeister-Boltenstern, Nitrous oxide emissions from soils: how well do we understand the processes and their controls?, *Philosophical Transactions of the Royal Society B: Biological Sciences*, 2013, **368**, 20130122.
25. D. Fowler, M. Coyle, U. Skiba, M. A. Sutton, J. N. Cape, S. Reis, L. J. Sheppard, A. Jenkins, B. Grizzetti, J. N. Galloway, P. Vitousek, A. Leach, A. F. Bouwman, K. Butterbach-Bahl, F. Dentener, D. Stevenson, M. Amann and M. Voss, The global nitrogen cycle in the twenty-first century, *Philosophical transactions of the Royal Society of London. Series B, Biological sciences*, **368**, 20130164-20130164.
26. S. J. Hall, W. H. McDowell and W. L. Silver, When Wet Gets Wetter: Decoupling of Moisture, Redox Biogeochemistry, and Greenhouse Gas Fluxes in a Humid Tropical Forest Soil, *Ecosystems*, 2013, **16**, 576-589.
27. A. H. Krichels, E. Sipic and W. H. Yang, Iron Redox Reactions Can Drive Microtopographic Variation in Upland Soil Carbon Dioxide and Nitrous Oxide Emissions, *Soil Systems*, 2019, **3**, 60.
28. H. Tian, R. Xu, J. G. Canadell, R. L. Thompson, W. Winiwarter, P. Suntharalingam, E. A. Davidson, P. Ciais, R. B. Jackson, G. Janssens-Maenhout, M. J. Prather, P. Regnier, N. Pan, S. Pan, G. P. Peters, H. Shi, F. N. Tubiello, S. Zaehle, F. Zhou, A. Arneth, G. Battaglia, S. Berthet, L. Bopp, A. F. Bouwman, E. T. Buitenhuis, J. Chang, M. P. Chipperfield, S. R. S. Dangal, E. Dlugokencky, J. W. Elkins, B. D. Eyre, B. Fu, B. Hall, A. Ito, F. Joos, P. B. Krummel, A. Landolfi, G. G. Laruelle, R. Lauerwald, W. Li, S. Lienert, T. Maavara, M. MacLeod, D. B. Millet, S. Olin, P. K. Patra, R. G. Prinn, P. A. Raymond, D. J. Ruiz, G. R. van der Werf, N. Vuichard, J. Wang, R. F. Weiss, K. C. Wells, C. Wilson, J. Yang and Y. Yao, A comprehensive quantification of global nitrous oxide sources and sinks, *Nature*, 2020, **586**, 248-256.
29. M. Wang, R. Hu, R. Ruser, C. Schmidt and A. Kappler, Role of Chemodenitrification for N2O Emissions from Nitrate Reduction in Rice Paddy Soils, *ACS Earth and Space Chemistry*, 2020, **4**, 122-132.
30. M. K. Jarecki, J. L. Hatfield and W. Barbour, Modeled Nitrous Oxide Emissions from Corn Fields in Iowa Based on County Level Data, *Journal of Environmental Quality*, 2015, **44**, 431-441.
31. C. S. Li, Modeling Trace Gas Emissions from Agricultural Ecosystems, *Nutrient Cycling in Agroecosystems*, 2000, **58**, 259-276.
32. J. M. Otte, N. Blackwell, V. Soos, S. Rughöft, M. Maisch, A. Kappler, S. Kleindienst and C. Schmidt, Sterilization impacts on marine sediment---Are we able to inactivate microorganisms in environmental samples?, *FEMS Microbiol Ecol*, 2018, **94**.
33. R. M. S. U. Cornell and U. Schwertmann, *The Iron Oxides: Structure, Properties, Reactions, Occurrences, And Uses*, 2003.

34. C. A. Gorski and M. M. Scherer, Influence of Magnetite Stoichiometry on FeIIUptake and Nitrobenzene Reduction, *Environmental Science & Technology*, 2009, **43**, 3675-3680.
35. P. Larese-Casanova and M. M. Scherer, Fe(II) Sorption on Hematite: New Insights Based on Spectroscopic Measurements, *Environmental Science & Technology*, 2007, **41**, 471-477.
36. L. Notini, D. E. Latta, A. Neumann, C. I. Pearce, M. Sassi, A. T. N'Diaye, K. M. Rosso and M. M. Scherer, The Role of Defects in Fe(II)-Goethite Electron Transfer, *Environ Sci Technol*, 2018, **52**, 2751-2759.
37. C. A. Gorski and M. M. Scherer, Determination of nanoparticulate magnetite stoichiometry by Mössbauer spectroscopy, acidic dissolution, and powder X-ray diffraction: A critical review, *American Mineralogist*, 2010, **95**, 1017-1026.
38. E. A. Bettis III, Late Wisconsinan and Holocene Alluvial Stratigraphy, Paleoecology, and Archeological Geology of East -central Iowa, *Iowa Department of Natural Resources*, 1992, **Geological Survey Bureau**.
39. K. E. Schilling, Y. K. Zhang and P. Drobney, Water table fluctuations near an incised stream, Walnut Creek, Iowa, *Journal of Hydrology*, 2004, **286**, 236-248.
40. S. Rahutomo, J. L. Kovar and M. L. Thompson, Varying redox potential affects P release from stream bank sediments, *PLOS ONE*, 2018, **13**, e0209208.
41. S. Rahutomo, J. L. Kovar and M. L. Thompson, Phosphorus transformations in stream bank sediments in Iowa, USA, at varying redox potentials, *Journal of Soils and Sediments*, 2019, **19**, 1029-1039.
42. S. Rahutomo, J. L. Kovar and M. L. Thompson, Inorganic and Organic Phosphorus in Sediments in the Walnut Creek Watershed of Central Iowa, USA, *Water, Air, & Soil Pollution*, 2018, **229**, 72.
43. K. E. Schilling, J. A. Palmer, E. A. Bettis Iii, P. Jacobson, R. C. Schultz and T. M. Isenhart, Vertical distribution of total carbon, nitrogen and phosphorus in riparian soils of Walnut Creek, southern Iowa, *Catena*, 2009, **77**, 266-273.
44. B. K. G. Theng, G. Lagaly, F. Bergaya, B. K. G. Theng and G. Lagaly, *Handbook of Clay Science*, Elsevier Science & Technology, Amsterdam, UNITED KINGDOM, 2006.
45. L. Heller-Kallai and I. Rozenson, The use of mössbauer spectroscopy of iron in clay mineralogy, *Physics and Chemistry of Minerals*, 1981, **7**, 223-238.
46. A. G. Ilgen, R. K. Kukkadapu, K. Leung and R. E. Washington, “Switching on” iron in clay minerals, *Environmental Science: Nano*, 2019, **6**, 1704-1715.
47. A. G. B. Williams and M. M. Scherer, Spectroscopic Evidence for Fe(II)−Fe(III) Electron Transfer at the Iron Oxide−Water Interface, *Environmental Science & Technology*, 2004, **38**, 4782-4790.
48. M. D. Dyar, D. G. Agresti, M. W. Schaefer, C. A. Grant and E. C. Sklute, MÖSSBAUER SPECTROSCOPY OF EARTH AND PLANETARY MATERIALS, *Annual Review of Earth and Planetary Sciences*, 2006, **34**, 83-125.
49. H. Dong, R. K. Kukkadapu, J. K. Fredrickson, J. M. Zachara, D. W. Kennedy and H. M. Kostandarithes, Microbial Reduction of Structural Fe(III) in Illite and Goethite, *Environmental Science & Technology*, 2003, **37**, 1268-1276.
50. L. Tuominen, T. Kairesalo and H. Hartikainen, Comparison of methods for inhibiting bacterial activity in sediment, *Applied and environmental microbiology*, 1994, **60**, 3454-3457.
51. *Journal*, 2012, **141.62**.
52. H. Tamura, K. Goto, T. Yotsuyanagi and M. Nagayama, Spectrophotometric determination of iron(II) with 1,10-phenanthroline in the presence of large amounts of iron(III), *Talanta*, 1974, **21**, 314-318.
53. L. A. Ridnour, J. E. Sim, M. A. Hayward, D. A. Wink, S. M. Martin, G. R. Buettner and D. R. Spitz, A Spectrophotometric Method for the Direct Detection and Quantitation of Nitric Oxide, Nitrite, and Nitrate in Cell Culture Media, *Analytical Biochemistry*, 2000, **281**, 223-229.

54. W. T. Bolleter, C. J. Bushman and P. W. Tidwell, Spectrophotometric Determination of Ammonia as Indophenol, *Analytical Chemistry*, 1961, **33**, 592-594.
55. N. M. Tzollas, G. A. Zachariadis, A. N. Anthemidis and J. A. Stratis, A new approach to indophenol blue method for determination of ammonium in geothermal waters with high mineral content, *International Journal of Environmental Analytical Chemistry*, 2010, **90**, 115-126.
56. P. Bénézeth, J. L. Dandurand and J. C. Harrichoury, Solubility product of siderite (FeCO3) as a function of temperature (25–250 °C), *Chemical Geology*, 2009, **265**, 3-12.
57. S. M. Stewart, T. B. Hofstetter, P. Joshi and C. A. Gorski, Linking Thermodynamics to Pollutant Reduction Kinetics by Fe2+ Bound to Iron Oxides, *Environmental Science & Technology*, 2018, **52**, 5600-5609.
58. A. M. Jones, P. J. Griffin, R. N. Collins and T. D. Waite, Ferrous iron oxidation under acidic conditions – The effect of ferric oxide surfaces, *Geochimica et Cosmochimica Acta*, 2014, **145**, 1-12.
59. P. A. Cárdenas-Hernández, K. A. Anderson, J. Murillo-Gelvez, D. M. Di Toro, H. E. Allen, R. F. Carbonaro and P. C. Chiu, Reduction of 3-Nitro-1,2,4-Triazol-5-One (NTO) by the Hematite–Aqueous Fe(II) Redox Couple, *Environmental Science & Technology*, 2020, **54**, 12191-12201.
60. D. E. Latta, C. A. Gorski, M. I. Boyanov, E. J. O'Loughlin, K. M. Kemner and M. M. Scherer, Influence of Magnetite Stoichiometry on UVI Reduction, *Environmental Science & Technology*, 2012, **46**, 778-786.
61. C. A. Gorski, J. T. Nurmi, P. G. Tratnyek, T. B. Hofstetter and M. M. Scherer, Redox Behavior of Magnetite: Implications for Contaminant Reduction, *Environmental Science & Technology*, 2010, **44**, 55-60.
62. T. S. Pasakarnis, M. I. Boyanov, K. M. Kemner, B. Mishra, E. J. O'Loughlin, G. Parkin and M. M. Scherer, Influence of chloride and Fe(II) content on the reduction of Hg(II) by magnetite, *Environ Sci Technol*, 2013, **47**, 6987-6994.
63. J. Entwistle, D. E. Latta, M. M. Scherer and A. Neumann, Abiotic Degradation of Chlorinated Solvents by Clay Minerals and Fe(II): Evidence for Reactive Mineral Intermediates, *Environmental Science & Technology*, 2019, **53**, 14308-14318.
64. K. E. Schilling, E. McLellan and E. A. Bettis, Letting Wet Spots be Wet: Restoring Natural Bioreactors in the Dissected Glacial Landscape, *Environmental Management*, 2013, **52**, 1440-1452.
65. M. D. Tomer, K. E. Schilling and K. J. Cole, Nitrate on a Slow Decline: Watershed Water Quality Response during Two Decades of Tallgrass Prairie Ecosystem Reconstruction in Iowa, *Journal of Environmental Quality*, 2019, **48**, 579-585.
66. M. F. Helmke, W. W. Simpkins and R. Horton, Fracture-Controlled Nitrate and Atrazine Transport in Four Iowa Till Units, *Journal of Environmental Quality*, 2005, **34**, 227-236.
67. K. S. Pfenning and P. B. McMahon, Effect of nitrate, organic carbon, and temperature on potential denitrification rates in nitrate-rich riverbed sediments, *Journal of Hydrology*, 1997, **187**, 283-295.